2011 American Control Conference
on O'Farrell Street, San Francisco, CA, USA
June 29 - July 01, 2011

# Controller Design for Nonlinear Systems Using the Robust Controller Bode (RCBode) Plot

J.D. Taylor and William Messner

*Abstract*— **In this paper, we develop a controller design method for nonlinear systems using the Robust Controller Bode (RCBode) plot. A robust performance criterion defines allowed and forbidden regions for the controller frequency response on the RCBode plot. The nonlinear system is linearized about a finite set of operating points which are considered to be a set of structured uncertainties. The union of the forbidden regions of each linearized system then defines the RCBode plot of the nonlinear system. We apply an iterative loop shaping technique to eliminate the intersections between the forbidden regions of the RCBode plot and the frequency response of the controller. We demonstrate the effectiveness of this technique for the design of a flow-rate controller for a dynamic nonlinear butterfly valve system. We show that this design is less conservative than a design satisfying the Circle Criterion. Finally, simulations are presented which verify the performance of the compensated system.**

## I. INTRODUCTION

One of the most commonly used approaches to controller design for nonlinear systems is gain scheduling where individual linear controllers are designed for the linearized dynamics of the nonlinear system at various operating points [1]. A variation of this approach is the design of a single linear controller which simultaneously stabilizes the set of linearized plants. Simultaneous stabilization is the approach that we employ by considering the set of linearized dynamics to be a set of structured uncertainties.

Automated design tools such as $H_\infty$ and $\mu$-synthesis methods are widely used for synthesizing robust controllers for systems with structured uncertainties [2]; however, since these approaches are based on mathematical optimization procedures, they do not provide the designer with much insight into the relationship between open-loop frequency response and performance. Also these tools require that the plant, the uncertainty weighting functions, and the performance weighting functions all be represented by realizable transfer functions. Construction of these transfer functions themselves can be quite difficult. For SISO systems these automated approaches often trade the difficulty of controller synthesis for the difficulty of construction of weighting functions and plant models; consequently, designs that are more conservative than necessary may result. Approaches based on Quantitative Feedback Theory (QFT) [3], can represent the plant and uncertainties as frequency response data alone; however, QFT employs the Nichols chart, for which frequency is a parametric variable and, therefore, hidden.

The authors are with the Department of Mechanical Engineering, Carnegie Mellon University, Pittsburgh, PA 15213 jdtaylor@andrew.cmu.edu, bmessner@andrew.cmu.edu

The Robust Bode (RBode) plot was developed to provide an intuitive visual approach to robust controller synthesis for unstructured uncertainties [4]. The robust performance criterion is represented as allowed and forbidden regions on the Bode magnitude and phase charts for the open-loop frequency response of the controller and plant. Realizable transfer function models are *not* required for the plant model or the weighting functions – frequency response data alone is sufficient. The strategy for compensator design with the RBode plot is to shape the controller frequency response to eliminate all intersections with the forbidden regions at all frequencies. By employing the Bode plot, frequency is explicitly shown, making controller selection much easier than with QFT.

The RBode plot can still result in unnecessarily conservative designs because all uncertainties are considered to be unstructured uncertainties (i.e. no phase information). The Robust Controller Bode (RCBode) plot is a variation of the RBode plot developed to address these limitations when designing for *structured* uncertainties [5]. These structured uncertainties are represented as a set of frequency responses with both magnitude and phase information available.

To demonstrate this approach we consider the problem of fluid flow-rate control with a butterfly valves. The control of fluid flow-rate is a critical engineering challenge in a wide variety of applications, for example in the chemical processing industry and in various cooling systems. Butterfly valves are common control components in these systems due to their relatively quick response time and wider throttling range compared to other valve types; however, in butterfly valves the flow-rate is a highly nonlinear function of valve angle [6]; therefore, any controller for this system must be designed to ensure robust stability and performance in the presence of this nonlinearity as well as any additional disturbances which may arise due to the uncertain dynamics of the flow.

## II. SYSTEM MODEL AND LINEARIZATION

The block diagram describing the flow-rate feedback control system is shown in Fig. 1, where $C(s)$ is the controller transfer function, $M(s)$ is the geared motor transfer function, $\Phi$ is the valve nonlinearity, $P_n(s)$ is the linearized plant transfer function at the $n^{th}$ operating point, $r$ is the reference flow-rate, $y$ is the output flow-rate, and $d$ is the disturbance signal.

978-1-4577-0079-8/11/$26.00 ©2011 AACC

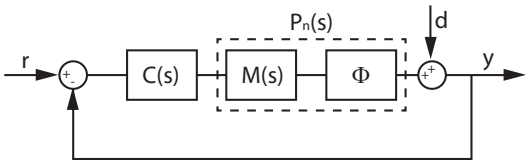


Fig. 1. Block diagram of nonlinear valve system.

### A. Geared DC Electric Motor Model

The dynamics of the geared DC electric motor are represented by the differential equations (1)-(2).

$$J\ddot{\theta}(t) + b\dot{\theta}(t) = NK_\tau i(t) \tag{1}$$

$$L\frac{di}{dt} + Ri(t) = v(t) - NK_\tau\dot{\theta}(t) \tag{2}$$

where $\theta(t)$ and $\dot{\theta}(t)$ are the valve angle and angular velocity, $i(t)$ is the current, and $v(t)$ is the applied voltage. The transfer function from voltage input to valve angle output is given in Eq. (3).

$$M(s) = \frac{\Theta(s)}{V(s)} = \frac{NK_\tau}{s[(Js+b)(Ls+R)+(NK_\tau)^2]} \tag{3}$$

The constant parameters and their values are defined in Table I.

TABLE I

| Geared DC Motor Parameters | |
|---|---|
| Motor Torque Constant | $K_\tau$ =1E-4 N-m/A |
| Motor Coil Resistance | $R = 200\ \Omega$ |
| Motor Coil Inductance | $L = 0.03$ H |
| Motor-Gearbox-Load Inertia | $J = 0.04$ kg-m$^2$ |
| Motor-Gearbox-Load Viscous Damping | $b = 0.07$ N-m/s |
| Gearbox Gear Ratio | $N = 25$ |

### B. Butterfly Valve Model

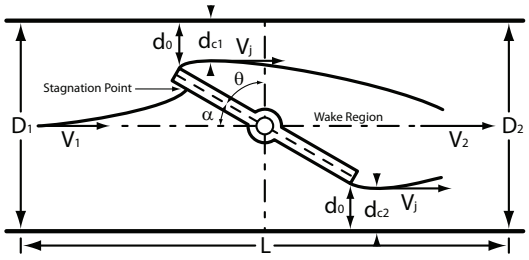


Fig. 2. Schematic Diagram of Butterfly Valve Flow.

The nonlinear mapping from valve opening angle to volumetric flow-rate through a butterfly valve was derived in [6] and is given in Eq. (4). Note that $\theta = 0°$ corresponds to a closed valve with no flow and $\theta = 90°$ to an open valve with maximum flow.

$$Q = \Phi(\theta) = \left(\frac{2\Delta P D^2}{\rho(\zeta_e + \zeta_f)}\right)^{1/2} \tag{4}$$

where $Q$ is the volumetric flow-rate, $\Delta P$ is the pressure drop across the valve, $D$ is the valve diameter, $\rho$ is the fluid density, and $\zeta_e$ and $\zeta_f$ are the dimensionless pressure loss coefficients due to flow expansion and pipe friction respectively.

$$\zeta_e = \left(\frac{2}{(C_{c1}+C_{c2})(1-\cos(\theta))} - 1\right)^2 \tag{5}$$

$$\zeta_{f_{laminar}} = \frac{64\mu L}{\rho V D^2} \tag{6}$$

where $C_{c1}$ and $C_{c2}$ are the coefficients of contraction, $\mu$ is the fluid dynamic viscosity, $L$ is the length of the pipe segment containing the butterfly valve, and $V$ is the fluid velocity. Because the coefficient, $\zeta_f$, is a function of flow-rate ($V = Q/A$), the relation in Eq. (4) is implicit, and some root finding procedure is typically necessary. The flow-rate is shown as a function of valve angle in Fig. 3.

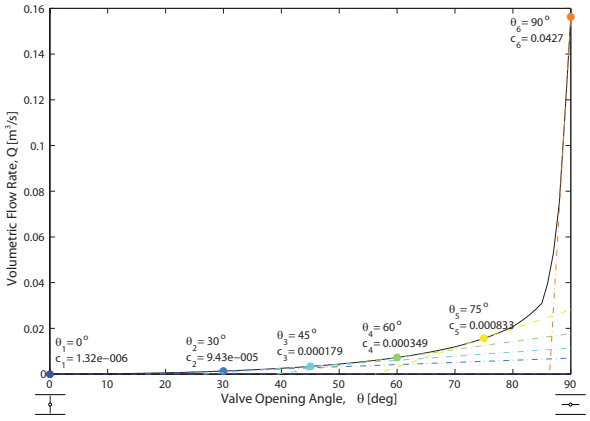


Fig. 3. Flow-rate as function of valve angle and linearizations about several operating points.

### C. Linearized System Model

The nonlinear dynamical system $\dot{x} = f(x,u), \quad y = g(x)$ may be linearized about an equilibrium operating point $(x_0, u_0) : \dot{x} = f(x_0, u_0) = 0$ as follows:

$$\delta\dot{x} \approx \nabla_x f|_{(x_0,u_0)}\delta x + \nabla_u f|_{(x_0,u_0)}\delta u = A\cdot\delta x + B\cdot\delta u$$

$$\delta y = y - g(x_0) \approx \nabla_x g|_{(x_0)}\delta x = C\cdot\delta x \tag{7}$$

The linearized transfer function of the nonlinear dynamical system in the neighborhood of $(x_0, u_0)$ is therefore, $P_0(s) = C(sI - A)^{-1}B$. Since the valve introduces only a static nonlinearity to the system output (i.e. $y = g(x) = \Phi(\theta)$), and the dynamics of the motor are essentially linear, the linearizations of this system are relatively trivial, Eq. (8).

$$P_n(s) = \frac{E(s)}{V(s)} = \frac{c_n NK_\tau}{s[(Js+b)(Ls+R)+(NK_\tau)^2]} \tag{8}$$

$$c_n = \left.\frac{d\Phi}{d\theta}\right|_{\theta_n} \tag{9}$$

The fluid flow-rate, $Q$ as a function of valve angle, $\theta$, is shown in Fig. 3, along with the linearization about a few representative operating points. The linearized open-loop transfer functions evaluated at these operating points are provided in Fig. 4.

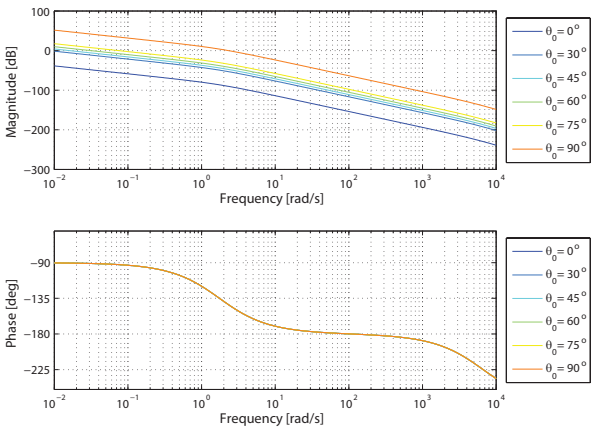


Fig. 4. Linearized open-loop transfer functions evaluated at several operating points.

## III. UNCERTAINTY, ROBUST PERFORMANCE, AND RCBODE PLOTS

Any mathematical model of a physical system will have characteristics which are not accurately represented by that model. These unmodeled characteristics broadly fall into two categories 1) Structured uncertainty and 2) Unstructured uncertainty [2]. The structured uncertainty could for instance be given by a discrete set of plants. It is structured in the sense that there is accurate gain and phase bounds as a function of frequency. Often the structured uncertainty is the result of variations in the plant parameters over the operating range, for instance in our nonlinear valve system.

The unstructured uncertainty is representative of unmodeled and stochastic processes, for instance noise in the measured signals. It is characterized by only gain information, and as such may be represented by a disc uncertainty in the complex plane. Unstructured uncertainties must increase in magnitude with frequency since at some frequency all phase knowledge is lost, (i.e. phase uncertainty is $\pm 180$).

The overall multiplicative uncertainty, $\Delta_m$, in the system depends on the structured uncertainty, $\Delta_s$, and unstructured uncertainty, $\Delta_u$, as in Eq. (10). A block diagram showing how these uncertainties enter the system is provided in Fig. 5.

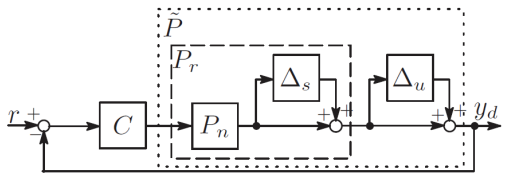


Fig. 5. Block diagram illustrating structured and unstructured uncertainties

$$|\Delta_m(\omega)| = |\Delta_s(\omega)| + |\Delta_u(\omega)| + |\Delta_s(\omega)||\Delta_u(\omega)| \quad (10)$$

### A. Uncertainty Weighting Functions

In robust controller design, two weighting functions are used which are related to the sensitivity, $S(\omega)$, and complementary sensitivity functions, $T(\omega)$. These functions are defined in the standard way.

$$S(\omega) = \frac{1}{1 + C(\omega)P(\omega)}, \quad T(\omega) = \frac{C(\omega)P(\omega)}{1 + C(\omega)P(\omega)} \quad (11)$$

The uncertainty weighting function, $W_u(\omega)$, is chosen to over-bound the multiplicative uncertainty magnitude at all frequencies.

$$|W_u(\omega)| > \max|\Delta_m(\omega)|, \quad \forall\omega \quad (12)$$

It can be shown that to achieve robust stability against $\Delta_m$ the complementary sensitivity function, $T(\omega)$, must satisfy Eq. (13).

$$|T(\omega)| < |W_u(\omega)|^{-1}, \quad \forall\omega \quad (13)$$

The sensitivity weighting function, $W_s(\omega)$, is chosen to meet frequency domain performance specifications for the closed-loop system, c.f. Section IV B.

$$|S(\omega)| < |W_s(\omega)|^{-1}, \quad \forall\omega \quad (14)$$

### B. Robust Performance Condition

Robust performance is achieved if every member of the uncertainty set satisfies Eq. (14). It can be shown that if the open-loop transfer function, $P(s)C(s)$ is stable then a necessary and sufficient condition for the robust performance of the closed-loop system is given by Eq. (15) [2].

$$|W_u(\omega)T(\omega)| + |W_s(\omega)S(\omega)| < 1, \quad \forall\omega \quad (15)$$

### C. Robust Controller (RCBode) Bode Plot

By substituting the open-loop magnitude $|C(s)||P(s)|$ and phase $\angle C(s) + \angle P(s)$ into the robust performance criteria Eq. (15), it is possible to derive conditions on the controller magnitude and phase.

Phase Criterion:

$$\cos(\angle C(j\omega) + \angle P(j\omega)) > Q(\omega), \quad \forall\omega \quad (16)$$

where

$$Q(\omega) = \frac{|W_s(\omega)|^2 - 1}{2|C(j\omega)||P(j\omega)|} + |W_u(\omega)||W_s(\omega)| + \frac{\left(|W_u(\omega)|^2 - 1\right)|C(j\omega)||P(j\omega)|}{2} \quad (17)$$

Gain Criterion:

$$(1-|W_u(\omega)|^2)|P_n(\omega)|^2|C(j\omega)|^2+ \\ +2(\cos(\angle C(j\omega)+\angle P(j\omega)|) \\ -|W_u(\omega)||W_s(\omega)|)|P_n(\omega)||C(j\omega)| \\ +1-|W_s(\omega)|^2>0, \quad \forall\omega. \quad (18)$$

The details of this derivation are presented in [4]. These conditions define allowed and forbidden regions for the controller frequency response that we call the Robust Controller Bode plot (RCBode). (See e.g. Figs. 7(a), 7(b), and 7(c)). The objective of loop-shaping controller design using the RCBode plot is to apply various compensators to shape the overall controller frequency response such that all intersections with the forbidden regions are eliminated at all frequencies.

## IV. LOOP-SHAPING CONTROLLER DESIGN WITH THE RCBODE PLOT

The controller design follows a four step process. Note that we are considering the union of the forbidden regions due to each linearized plant. It has been shown that this results in a less conservative design (i.e. smaller forbidden regions) than if a larger structured uncertainty is chosen to account for the variation of the plant parameters [5].

**Step 1** Determine the frequency response of the linearized plants $P_n$ and the weighting functions $W_u$ and $W_s$, all of which could be represented by either frequency response data or transfer functions.

**Step 2** Design an initial controller $C_0$ which stabilizes each $P_n$. Then plot the union of all RCBode plots for all linearized plants using $P_n$, $|W_u|$, $|W_s|$, and $C = C_0$.

**Step 3** Design the loop-shaping filter $C_s$ to satisfy the low frequency robust performance criteria on the first RCBode plot. Then plot the second RCBode plot using $P_n$, $|W_u|$, $|W_s|$, and $C = C_0C_s$.

**Step 4** Design the loop-shaping filter $C_u$ to satisfy the high frequency robust performance criteria on the second RCBode plot.

### A. Performance Specifications

1) Zero steady-state error for constant disturbance
2) Disturbance attenuation of at least -3 dB below 2 Hz
3) Maximum 6 dB disturbance amplification above 10 Hz

### B. Weighting Functions

The second and third performance specifications define bounds on the sensitivity function for the system. We choose the following sensitivity weighting function to meet those requirements.

$$|W_s(\omega)|^{-1} = \frac{2\omega}{\sqrt{\omega^2+12^2}} \quad (19)$$

The sensitivity weighting function and its inverse are shown in Fig. 6.

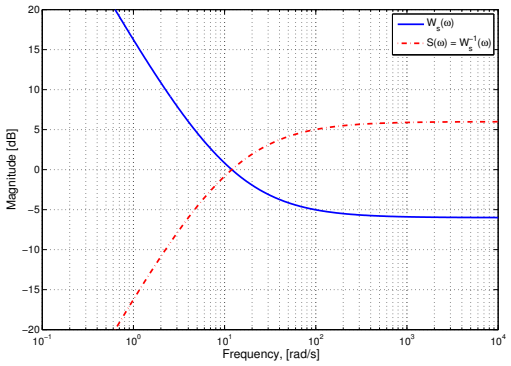


Fig. 6. Sensitivity and sensitivity weighting functions

Since we assume that our nonlinear model of the valve is accurate at frequencies below roughly $10^3$ rad/s, we choose the uncertainty weighting function to take the following form.

$$|W_u(\omega)| = \begin{cases} 0.01 & : x \le 10^3 \text{ rad/s} \\ 0.5 & : x > 10^3 \text{ rad/s} \end{cases} \quad (20)$$

## V. DESIGN ITERATIONS AND RESULTS

The open-loop system is already stable due to the pole at zero in the motor transfer function. We begin the controller design process by choosing a constant gain of $C_0 = 5\times10^{10}$. This choice yields the RCBode plot shown in Fig. 7(a). Note that we have increased the number of operating points to 240 equally spaced in the interval $\theta_n \in [30°, 90°]$ to smooth out the union of the forbidden regions on the RCBode plot.

The intersections of the controller frequency response with the forbidden regions (shown in grey) indicate that the constant gain controller violates the robust performance condition in the approximate frequency range 20 rad/s $< \omega < 10^3$ rad/s.

One option is to lift the controller phase over the phase forbidden region on the RCBode plot. To accomplish this, we may use the recently developed complex proportional-integral-lead compensator (CPIL) [7]. The structure of the CPIL transfer function is given in Eq. (21).

$$C_{cpil}(s) = \frac{s^2+2\zeta\omega_z s+\omega_z^2}{s(s+p)} \quad (21)$$

where

$$\omega_z = \omega_m\left(-\zeta\tan(\phi_m)+\sqrt{\zeta^2\tan^2(\phi_m)+1}\right), \quad (22)$$

$$p = \omega_m \sqrt{\frac{1 + sin\,(\phi_m)}{1 - sin\,(\phi_m)}}, \tag{23}$$

The phase contribution at $\omega_m$ is $\frac{3\phi_m}{2} - 45°$. The phase angle must satisfy $0 < \phi_m < 90°$. The zeros of this compensator are complex when $\zeta < 1$. Lower damping ratios provide higher gains at low frequencies and a steeper phase peak. Through a trial and error process the CPIL parameters were found to be $60°$ of phase added at $\omega_m = 7$ rad/s and damping ratio $\zeta = 0.7$.

The RCBode plot for the cascaded constant gain and CPIL compensators is shown in Fig. 7(b). It may appear that the center frequency of the CPIL compensator is too low; however, this is necessary when the final stage of the controller is added.

There are still intersections with the forbidden regions on the RCBode plot after application of the CPIL compensator in Fig. 7(b). We now add a final complex lead compensator defined by the transfer function in Eq. (24).

$$C_{clead} = \frac{\omega_p}{\omega_z}\left(\frac{s^2 + 2\zeta\omega_z s + \omega_z^2}{s^2 + 2\zeta\omega_p s + \omega_p^2}\right) \tag{24}$$

where $\omega_p = \omega_m(\zeta \tan(\phi) + \sqrt{\zeta^2 \tan^2(\phi) + 1}$ and $\omega_z = \omega^2/\omega_p$, and $\phi = \text{max phase}/2$. The parameters used here were max phase $= 50$ rad/s at $\omega_m = 1000$ rad/s and damping ratio $\zeta = 1.5$.

In the final RCBode plot, Fig. 7(c), all intersections with the forbidden regions have been eliminated indicating that the robust performance criterion is satisfied at all frequencies.

## VI. COMPARISON WITH CIRCLE CRITERION

The well known Circle Criterion provides a method for determining the stability of a nonlinear feedback system of the form given in Fig. 8, where $L(s)$ is the transfer function of a linear time invariant (LTI) system and $\Psi(\cdot)$ is a memory-less and possibly time-varying sector nonlinearity. The nonlinearity is said to belong to the sector $[\alpha, \beta]$, if for any input $u$ to $\Psi(\cdot)$, $\alpha u^2 \leq u\Psi(u) \leq \beta u^2$. The details of the circle criterion for different sector conditions can be found in [8]. The butterfly valve nonlinearity satisfies such a sector condition.

For $\beta > \alpha \geq 0$ the Circle Criterion states that a sufficient (but not necessary) condition for the stability of a nonlinear system is that the Nyquist plot of the open-loop frequency response, $L(j\omega)$, remains outside of a disc centered on and intersecting the real axis at $[\frac{-1}{\alpha}, \frac{-1}{\beta}]$.

Just as the robust performance condition Eq. (15) was used to define allowed and forbidden regions for the controller frequency response in RCBode, the circle criterion can be mapped onto the Bode plot of the controller frequency response. We call this the Circle Criterion Controller Bode (CCBode) plot. Any intersections of the controller magnitude and phase with the forbidden regions on the CCBode plot indicates that the open-loop system violates the circle criterion. We must emphasize here that an intersection does not mean that the system in unstable.

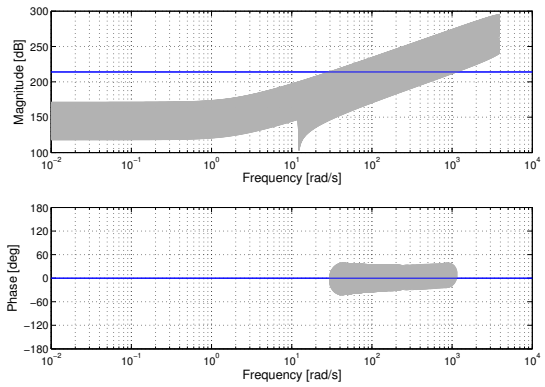


(a)

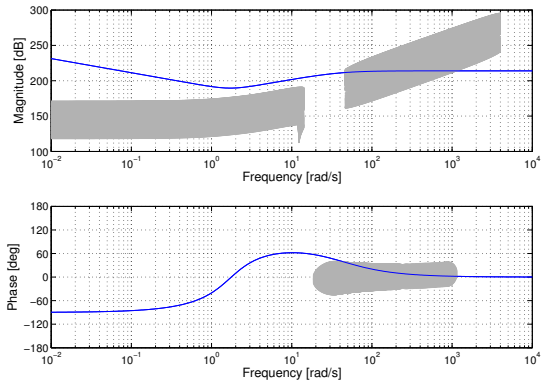


(b)

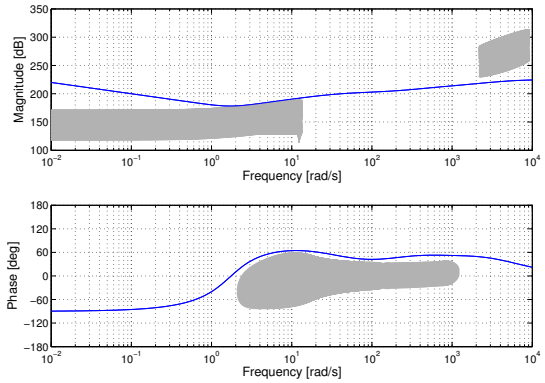


(c)

Fig. 7. Design Iterations on RCBode Plots (a) Constant gain (b) Constant gain + complex-proportional-integral-lead (CPIL) compensator, (c) Constant gain + CPIL + complex-lead (Clead) compensators. In the final iteration, all intersections with the forbidden regions have been eliminated indicating that the robust performance criterion is satisfied at all frequencies.

The CCBode plot of the controller designed using RCBode is given in Fig. 9. The intersections with the forbidden regions on the CCBode plot are consistent with the Nyquist plot and indicate that the robust performance condition is *less conservative* than the circle criterion and thus may be the preferred choice for robust controller design in many applications.

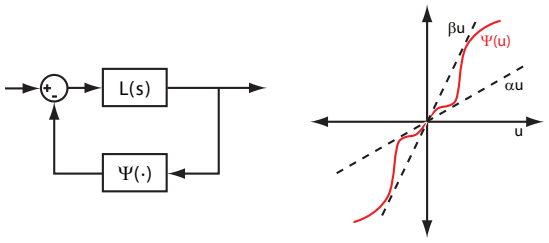


(a) (b)

Fig. 8. (a) Block diagram of system with linear part $L(s)$ and memory-less nonlinearity, $\Psi(\cdot)$. (b) An example of a nonlinear function belonging to the sector $[\alpha, \beta]$.

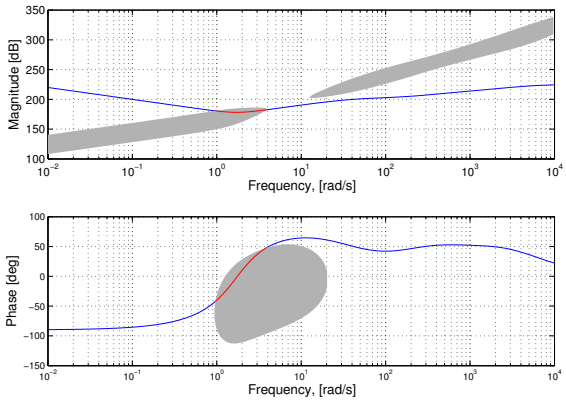


Fig. 9. CCBode plot of RCBode controller. The intersections with the forbidden regions indicate that the robust performance condition is less conservative than the circle criterion.

## VII. SIMULATIONS AND PERFORMANCE EVALUATIONS

Matlab Simulink© was used to simulate the time-domain response of the compensated motor-valve feedback system. The time-domain response of the compensated close-loop valve system to a step change in the reference flow-rate is presented in Fig. 10. Note that the full range of both the available flow-rate and valve angle are shown on the y-axis of the simulations illustrating the nonlinearity of the system. The simulations verify that the compensated system designed using the RCBode techniques does in fact meet the performance requirements, exhibiting stability in the face of the valve nonlinearity and settling time under 0.15 s.

## VIII. CONCLUSION

We developed a method for controller design for nonlinear systems using a modification of the Robust Bode plot called the Robust Controller Bode (RCBode) plot. The nonlinear system was linearized about a finite set of operating points, and this set of linearized dynamics was considered to be a set of structured uncertainties. The union of the forbidden regions for the frequency responses of the linearized dynamics for the Robust Bode plot of the controller defines the RCBode plot. We then applied an iterative loop shaping

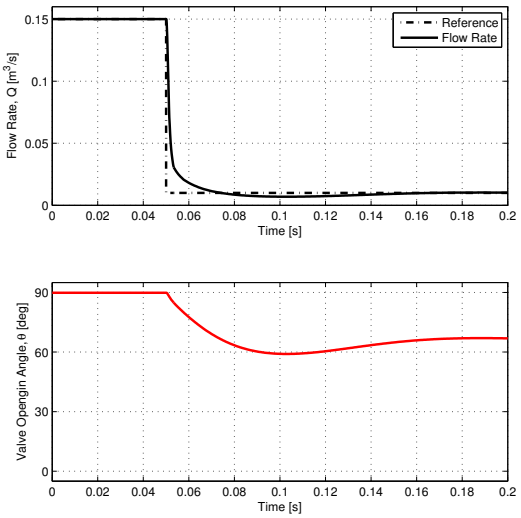


Fig. 10. Time-Domain simulation of compensated nonlinear valve system to step input.

technique to eliminate the intersections between the forbidden regions of the RCBode plot and the frequency response of the controller. We demonstrated the effectiveness of this technique for the design of a flow-rate controller for the nonlinear dynamic butterfly valve system. We showed that this design is less conservative than a design satisfying the Circle Criterion and verified the performance of the design in simulation.

## REFERENCES

[1] D. Leith and W. Leithead, "Survey of gain-scheduling analysis and design," *International Journal of Control*, vol. 73, no. 11, pp. 1001–1025, 2000.

[2] D. Zhou, *Glover 1996. K. Zhou, JC Doyle and K. Glover Robust and optimal control*. Prentice-Hall, Englewood Cliffs, NJ, 1996.

[3] I. Horowitz, "Quantitative feedback theory(QFT)," pp. 2032–2037, 1988.

[4] L. Xia and W. Messner, "An improved version of the RBode plot," in *American Control Conference, 2008*, 2008, pp. 4940–4945.

[5] T. Atsumi and W. Messner, "Modified Bode Plots for Head-Positioning Control in Hard Disk Drives with Structured and Unstructured Uncertainties," 13-15 Sep 2010, Boston, MA.

[6] J. Taylor, B. Sinopoli, and W. Messner, "Nonlinear modeling of butterfly valves and flow rate control using the Circle Criterion Bode plot," in *American Control Conference (ACC), 2010*. IEEE, 2010, pp. 1967–1972.

[7] W. Messner, "Classical control revisited: variations on a theme," *AMC '08. 10th IEEE International Workshop*, pp. 15–20, March 26-28 2008.

[8] H. Khalil, *Nonlinear systems*. Prentice-Hall, 2001.